RPE | Radiation Physics & Engineering
An International Peer-Reviewed Journal
Published by K.N. Toosi University of Technology
http://rpe.kntu.ac.ir
Research Article

Radiation Physics and Engineering 2022; 3(2):7–10
https://doi.org/10.22034/RPE.2022.335334.1062

Synthesis of hydroxyapatite through a solid-state reaction method and study of its thermoluminesence dosimetric properties against gamma rays

Parisa Taghipour[a], Farhad Zolfagharpour[a], Hamideh Daneshvar[b,*]

[a] *Department of Physics, Faculty of Sciences, University of Mohaghegh Ardabili, P.O. Box 179, Ardabil, Iran*
[b] *Radiation Application Research School, Nuclear Science & Technology Research Institute, P.O. Box 11365-3486, Tehran, Iran*

HIGHLIGHTS

- HAP samples synthesized via a solid-state reaction method to investigate the annealing effect on HAP structure.
- The synthesized samples are a combination of different crystal phases and an extera β-TCP phase.
- Among all synthesized samples, the TL response of the HAP-900 was higher than others.
- The linearity, fading effect and reproducibility of the samples were investigated.

ABSTRACT

In this research work, powder hydroxyapatite samples were synthesized using a solid-state reaction method to investigate the annealing effect. The crystal structure was carried out by XRD system produced data, and the Rietveld method using MAUD software. The samples were irradiated in different radiation absorbed doses up to 1500 Gy and their thermoluminescence properties including glow curve, response, fading effect and reproducibility were investigated from dosimetry point of view. The results showed that the annealing temperature significantly affects the crystal structure and thermoluminescence dosimetry response of hydroxyapatite samples, consequently. It was concluded that high temperature annealing process can lead to formation of β-TCP crystal phase during the synthesis of hydroxyapatite. Percentage of this formed phase increases with rising the temperature, and finally leads to increasing of the thermoluminescence response. It was concludded that in the solid state reaction method to increasing the TL response, it is better to use high annealing temperature for the synthesis of hydroxyapatite sample.

KEYWORDS

Hydroxyapatite
Solid state
Thermoluminescence
Dosimetry
Rietveld refinement

HISTORY

Received: 27 March 2022
Revised: 29 April 2022
Accepted: 2 May 2022
Published: Spring 2022

1 Introduction

Thermoluminescence (TL) is thermally stimulated emission of light from a semiconductor or insulator, following the previous absorption of energy from ionizing radiation such as X-rays, gamma rays, UV lights, *etc* (Fukuda et al., 1993). TL application in high radiation dosimetry, dating techniques in archaeology and geology and as well as the study of lattice defects continues to attract a wide attention of researchers (Bhatt and Kulkarni, 2014). For dosimetry applications a TL material is expected to have the following characteristics: relatively simple glow curve with the main peak at about 200 °C, high sensitivity, and stability (low fading), resistance to environmental factors and good linearity in the specific useful range of dose. A few materials have been found to match all the above characteristics (Azorin, 2014). Biomaterials are the most well-known proposals for TL dosimetry (Alvarez et al., 2014). One of these known materials is in the bones of the human body which its main content is hydroxyapatite (HAP) (Daneshvar et al., 2020).

This substance has been used as a high dose dosimeter, accident dosimeter, and the aging studies using EPR, TL, and OSL methods (Shafaei et al., 2016). HAP is one of the most important calcium phosphate compounds, 90 to 95% of enamel, 70 to 75% of tooth bone, and 60 to 70% of body bones. HAP is used at the nanoscale for drug delivery, biological probes, and bioimaging (Li et al., 2017).

HAP can be extracted from natural sources or synthesized chemically. Natural HAP is usually extracted from biological sources or wastes such as mammalian bone, marine or aquatic sources (e.g. fishbone and fish scale), shell sources (e.g. cockle, clam, eggshell, and seashell), plants, algae, and also from mineral sources (Pu'ad et al.,

*Corresponding author: hdaneshvar@aeoi.org.ir

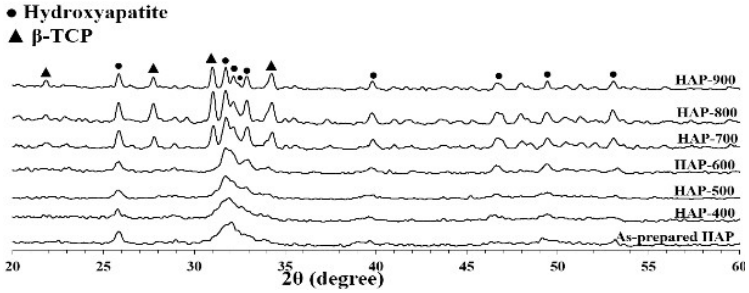

Figure 1: XRD patterns of final products.

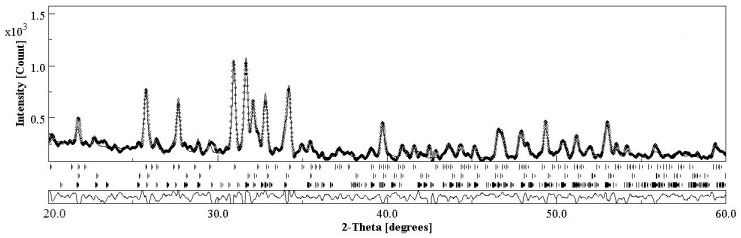

Figure 2: Rietveld refinement results using MAUD for synthesized HAP-900. Dots show the experimental and the solid line shows calculated results.

2019). Synthetic HAP can be fabricated through dry methods (e.g., solid-state reaction and mechanochemical), wet methods (e.g., chemical precipitation, hydrolysis, sol-gel, hydrothermal, emulsion, and sonochemical), and high-temperature processes (e.g. combustion and pyrolysis) (Sadat-Shojai et al., 2013). Compared to synthetic HAP, natural HAP is non-stoichiometric.

HAP can exist in two crystal forms of hexagonal and monoclinic or a combination of both (Haverty et al., 2005). The space group for the hexagonal structure of HAP is $P6_3/m$, with the lattice parameters of $a = b = 9.432$ Å, $c = 6.881$ Å and the space group for the monoclinic structure of HAP is $P2_1/b$, with the lattice parameters of $a = 9.421$ Å, $b = 2a$, $c = 6.881$ Å, and $\gamma = 120°$ (Pérez-Solis et al., 2018).

In our previous work, HAP was synthesized through hydrolysis and hydrothermal method to investigate the effect of phase structure of HAP on TL response. It was observed that an extra β-TCP phase is formed during synthesis of HAP, which leads to an increase in the TL response (Taghipour et al., 2022). In the present work, HAP powder was synthesized via solid-state reaction method to investigate the effect of annealing temperature on the phase structure of HAP and also on its TL properties.

2 Experimental: Preparation of the materials

In this method, $Ca(NO_3)_2.4H_2O$ (99% Merck), $(NH_4)_2HPO_4$ (99% Merck) and $NaHCO_3$ (99% Merck) were used as the starting materials, which were combined at room temperature. Ca/P ratio of 1.67, which is the stoichiometric Ca/P ratio in HAP, was kept constant. The reactants were ground and then blended. Grinding was continued until a foamy white liquid formed. After 24 h aging, the resultant products were washed several times with ethanol and de-ionized water to complete removal of the by-products and then dried in an oven at 80 °C for 6 h. The dried sample was termed as As-prepared HAP and annealed HAP at 400, 500, 600, 700, 800, and 900 °C (for 3hr) are termed HAP-400, HAP-500, HAP-600, HAP-700, HAP-800 and HAP-900, respectively.

3 Results and discussion

3.1 XRD and Rietveld analyses

In this study, diffraction patterns were obtained using the STOE STADI-MP Diffractometer (40 mA at 40 kV) available at the Institute of Nuclear Science and Technology Research Institute (NSTRI), Iran, and Cuk radiation. Scanning was carried out in the 2θ range 20 to 60. Figure 1 shows the diffraction pattern of samples in 2θ range 20 to 60. Rietveld refinement was performed using MAUD software to calculate the percentage of formed crystal phases. It was found that samples are a combination of hexagonal and monoclinic and an extera β-TCP phase. CIF files required for MAUD came from the website of (http://crystallography.net/) with COD ID 7217892, 2300273, and 1517238 for the monoclinic, hexagonal and β-TCP phases, respectively. The result of the Rietveld refinement is shown in Fig. 2. As it can be observed from this figure, the experimental and the calculated patterns had a good agreement and diffraction peaks well matched. The obtained phase percentages using MAUD software are given in Table 1.

As it can be seen from Fig. 1 and Table 1, all of the samples are a combination of different crystal phases with a high percentage of hexagonal phase. Also, the HAP decomposes to β-TCP at 700 °C. β-TCP percentage increases with increasing temperature up to 800 °C and then

remains constant. This study showed that the final products never contained less than 50 wt% hexagonal HAP. A similar result was obtained by Morgan et al. for the monoclinic HAP (Morgan et al., 2000).

Scherer's formula used to calculate the average crystallite size according to Eq (1):

$$d = \frac{K\lambda}{B\,cos\theta} \quad (1)$$

where d is the average particle diameters in nm, K is the shape factor, B is the broadening of the diffraction line measured as the full width at the half-maximum intensity in radian, λ is the wavelength of Cu X-rays in nm, and θ is Bragg's angle. The average grain size in angle of 31.005° of 2θ was estimated as $\sim$ 30 nm.

3.2 Glow curve

Figure 3 demonstrates the effect of annealing temperature on TL glow curves of samples irradiated at 800 Gy using Co-60 gamma-cell 220 in Radiation Application Research School at doses up to 1500 Gy. The dose rate of this gamma-ray source was about 1.5 Gy.s^{-1}. The Harshaw TLD reader, model 4500 available at NSTRI was used in this work. The results showed that the HAP-900 have the highest area under curve with a main peak at 230 °C.

3.3 TL response

In this experiment, the TL response was assumed as the area under the glow curve. Figure 4 shows the response-dose curves for synthesized samples. The tests were repeated three times for each irradiation dose. Error bars are also given in terms of standard deviation in the figure.

According to the Figs. 3 and 4, HAP-900 sample has the highest area under the glow curve and consequently the highest TL response. It means that in solid-state reaction synthesis method, high annealing temperature and also existence of β-TCP phase are effective in improving the TL response. Also, the response is linear up to 1000 Gy and then saturated at 1500 Gy that means HAP synthesized in this study is appropriate for dosymetric purposes up to 1000 Gy.

3.4 Fading

To study the fading effect, samples irradiated to 800 Gy. The fading effects of samples were studied during 30 days after irradiation. The result is shown in Fig. 5

Table 1: Formed phase percentages (%).

sample	Monoclinic	Hexagonal	β-TCP
As-prepared	19.12	80	0.88
HAP-400	15.11	84	0.89
HAP-500	9.37	90	0.63
HAP-600	0.25	98	1.75
HAP-700	7	57	36
HAP-800	1	50	49
HAP-900	1	50	49

It was observed that the TL response of the HAP-900 decreases by about 19% during two weeks after irradiation and then remains constant for two next weeks. This sample has the lowest fading during 30 days. The optimal time between irradiation and reading is 30 days for HAP-900. The As-prepared HAP has the highest fading and loses about 90% of its initial response during 30 days. Therefore, HAP-900 is optimal sample in this study.

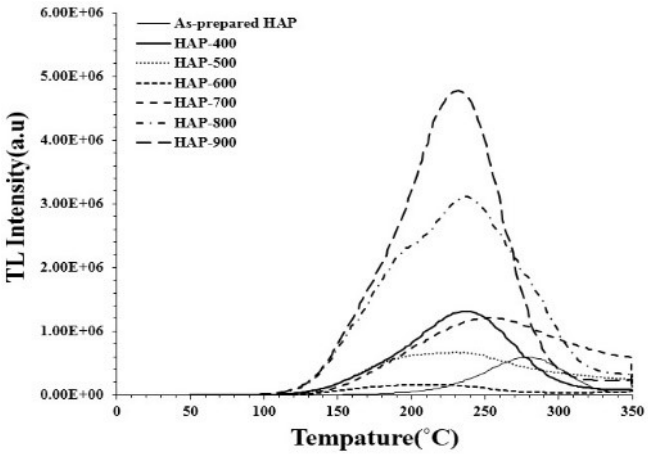

Figure 3: TL glow curves of the samples at 800 Gy.

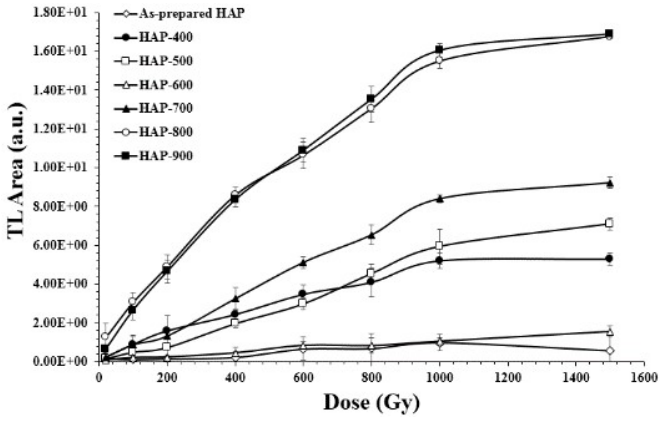

Figure 4: TL response of the samples at 800 Gy.

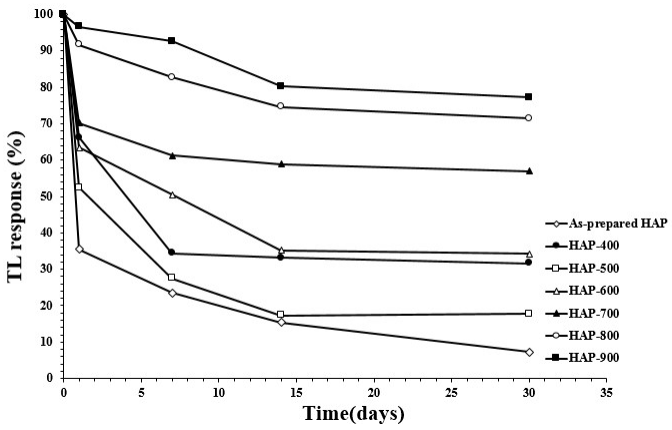

Figure 5: Fading effects of samples irradiated at 800 Gy during 30 days.

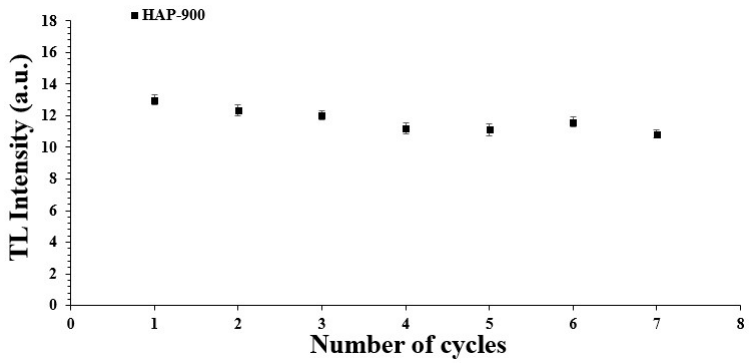

Figure 6: Reproducibility of HAP-900.

3.5 Reproducibility

Reproducibility test was done for optimal sample (i.e. HAP-900). The average TL responses along with their standard deviations after 7 successive cycles of thermal treatment at 400 °C, irradiation at 800 Gy and readout are presented in Fig. 6. The reproducibility of TL response was estimated less than ±5%.

According to Fig. 6, the TL response is aproximatly stable. Therefore, HAP-900 is appropriate from dosymetric point of viwe.

4 Conclusions

In this study, the HAP samples synthesized via a solid-state reaction method to investigate the annealing effect on HAP structure and TL properties. It was concluded from XRD and Rietvel analyses that the samples are a combination of different crystal phases with a high percentage of hexagonal phase and an extera β-TCP phase. HAP decomposes to β-TCP at 700 °C. β-TCP percentage increases with increasing temperature up to 800 °C and then remains constant. This study showed that the final products never contained less than 50 wt% hexagonal HAP. The average grain size using Scherer's formul in angle of 31.005° of 2θ was estimated as ∼30 nm.

Finally, the TL properties of the samples were studied. The TL response of the HAP-900 was higher than others. It was concluded that in the solid-state reaction method it is better to synthesis of HAP at high temperatures.

The linearity, fading effect and reproducibility of the samples were investigated and HAP-900 sample was determined as optimal sample and it was suitable for TL dosimetry up to 1000 Gy.

References

Alvarez, R., Rivera, T., Guzman, J., et al. (2014). Thermoluminescent characteristics of synthetic hydroxyapatite (SHAp). *Applied Radiation and Isotopes*, 83:192–195.

Azorin, J. (2014). Preparation methods of thermoluminescent materials for dosimetric applications: An overview. *Applied Radiation and Isotopes*, 83:187–191.

Bhatt, B. C. and Kulkarni, M. (2014). Thermoluminescent phosphors for radiation dosimetry. In *Defect and Diffusion Forum*, volume 347, pages 179–227. Trans Tech Publ.

Daneshvar, H., Shafaei, M., Manouchehri, F., et al. (2020). Influence of morphology and chemical processes on thermoluminescence response of irradiated nanostructured hydroxyapatite. *Journal of Luminescence*, 219:116906.

Fukuda, Y., Ohtaki, H., Tomita, A., et al. (1993). Thermoluminescence of hydroxyapatite doped with copper. *Radiation Protection Dosimetry*, 47(1-4):205–207.

Haverty, D., Tofail, S. A., Stanton, K. T., et al. (2005). Structure and stability of hydroxyapatite: Density functional calculation and Rietveld analysis. *Physical Review B*, 71(9):094103.

Li, H., Mei, L., Liu, H., et al. (2017). Growth mechanism of surfactant-free size-controlled luminescent hydroxyapatite nanocrystallites. *Crystal Growth & Design*, 17(5):2809–2815.

Morgan, H., Wilson, R., Elliott, J., et al. (2000). Preparation and characterisation of monoclinic hydroxyapatite and its precipitated carbonate apatite intermediate. *Biomaterials*, 21(6):617–627.

Pérez-Solis, R., Gervacio-Arciniega, J. J., Joseph, B., et al. (2018). Synthesis and characterization of a monoclinic crystalline phase of hydroxyapatite by synchrotron X-ray powder diffraction and piezoresponse force microscopy. *Crystals*, 8(12):458.

Pu'ad, N. M., Koshy, P., Abdullah, H., et al. (2019). Syntheses of hydroxyapatite from natural sources. *Heliyon*, 5(5):e01588.

Sadat-Shojai, M., Khorasani, M.-T., Dinpanah-Khoshdargi, E., et al. (2013). Synthesis methods for nanosized hydroxyapatite with diverse structures. *Acta Biomaterialia*, 9(8):7591–7621.

Shafaei, M., Ziaie, F., Sardari, D., et al. (2016). Thermoluminescence properties of gamma-irradiated nano-structure hydroxyapatite. *Luminescence*, 31(1):223–228.

Taghipour, P., Zolfagharpour, F., Daneshvar, H., et al. (2022). Thermoluminescence dose–response of synthesized and doped hydroxyapatite: effect of formed crystal phases. *Luminescence*.